

Synthesis and characterization of *N*-carbazole end-capped oligofluorenes

Vinich Promarak,* Sayant Saengsuwan, Siriporn Jungsuttiwong,
Taweesak Sudyoasuk and Tinnagon Keawin

Department of Chemistry, Faculty of Science, Ubon Ratchathani University, Warinchumrap, Ubon Ratchathani 34190, Thailand

Received 21 August 2006; revised 23 October 2006; accepted 1 November 2006

Available online 21 November 2006

Abstract—A series of *N*-carbazole end-capped oligofluorenes (CF_n , $n = 1-3$) were synthesized. The 9-position of the carbazole moiety was attached to the terminal ends of the oligofluorene cores using an Ullmann coupling reaction. These molecules exhibit red shifts in absorption and photoluminescence spectra with respect to the number of fluorene units and excellent electrochemical reversibility. They were found to be potential blue light-emitting or hole-transporting materials for organic light-emitting diodes (OLEDs). © 2006 Elsevier Ltd. All rights reserved.

A series of well-defined monodispersed oligofluorenes have recently attracted much attention as non-defect structural materials for electronic devices¹ and as important models to understand the fundamental properties of polyfluorenes (PF),² which are promising blue light-emitting materials for organic light-emitting diodes (OLEDs).³ The optical, thermal, and electrochemical properties of oligofluorenes have known to be changed by varying the substitution patterns at the 9-positions of the fluorenyl ring, by introduction of specific functional groups on the terminal ends of molecules or by incorporating oligofluorenes into different molecular architectures.⁴ Introduction of aryl pendant groups,⁵ chiral alkyl substituents⁶ or a spiro-configured structure⁷ to the 9-positions significantly improved the morphology and thermal stability of the oligofluorenes, while the electronic properties were retained. More recently, oligofluorenes end-capped with triarylamine-carbazole dendrons with very high thermal and electrochemical stabilities were reported.^{8,9} Due to its unique optical, electrical, and chemical properties, carbazole has been widely employed as a functional building block or substituent in the construction of organic photoconductors,¹⁰ non-linear optic (NLO) materials,¹¹ hole-transport and light-emitting materials for OLED devices¹² and host materials for phosphorescence appli-

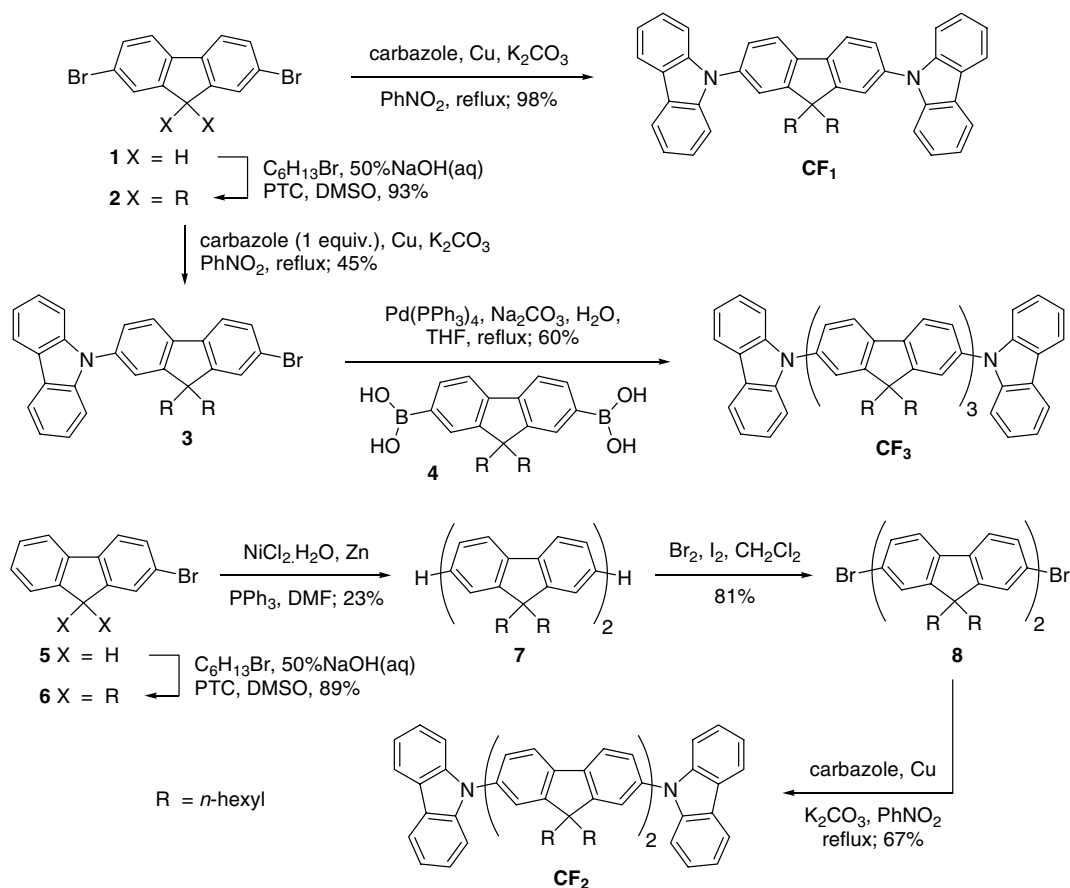
cations.¹³ Moreover, the thermal stability and glassy state durability of these organic molecules were found to be significantly improved upon incorporation of a carbazole moiety in the structure.¹⁴ To the best of our knowledge, there is no report on *N*-carbazole-end capped oligofluorenes.

In this letter, we report the synthesis of oligofluorenes ($n = 1-3$) bearing carbazole units at both ends and investigate their basic physical properties.

The synthetic strategy to the target *N*-carbazole end-capped oligofluorenes (CF_n , $n = 1-3$) is outlined in Scheme 1. 2,7-Dibromofluorene **1**¹⁵ was alkylated at the C-9 position with *n*-hexylbromide followed by coupling of the resultant bromide **2** with an excess of carbazole under Ullmann coupling conditions in the presence of Cu-bronze as catalyst and K_2CO_3 as a base to give the desired compound CF_1 as a white solid in quantitative yield. Under similar conditions but with only 1 equiv of carbazole, the intermediate 7-bromo-2-carbazole-9,9-bis-*n*-hexylfluorene **3** was isolated in 45% yield as a colorless solid. The ¹H NMR spectrum of mono-adduct **3** showed a characteristic doublet signal for 4-H and 5-H of the carbazole at δ 8.19 ppm ($J = 7.8$ Hz) and the non-equivalent 4'-H and 5'-H of fluorene were observed as two doublets at δ 7.89 ppm ($J = 7.8$ Hz) and δ 7.65 ppm ($J = 8.4$ Hz). Coupling of the resulting intermediate **3** with 9,9-bis-*n*-hexylfluorene-2,7-diboronic acid **4** under Suzuki cross-coupling reaction conditions using $\text{Pd}(\text{PPh}_3)_4$ as a catalyst and Na_2CO_3

Keywords: Oligofluorenes; Carbazole; Ullmann coupling; Organic light-emitting diode.

* Corresponding author. Tel.: +66 1 5930005; fax: +66 45 288379; e-mail: vpvich@sci.ubu.ac.th



Scheme 1. Synthetic route to the target molecules CF_n ($n=1-3$).

as a base in THF afforded the target CF_3 as a light yellow solid in 60% yield. 2-Bromofluorene was bis-alkylated at the C-9 position with *n*-hexylbromide and subsequently converted to a dimer via a Ni(0)-catalyzed homocoupling reaction with $NiCl_2 \cdot H_2O$, Zn powder, and PPh_3 as catalysts in DMF to give the fluorene dimer **7** in low yield. Selective bromination of the 2- and 7-positions using Br_2 followed by coupling with excess carbazole under similar Ullmann coupling conditions give the target CF_2 as a white solid in reasonable yield. Compounds CF_n ($n=1-3$) were fully characterized by standard spectroscopic methods.¹⁶

In order to understand the geometries and electronic properties of compounds CF_n ($n=1-3$), quantum chemical calculations were performed using the BLYP/6-31G** method. As illustrated in Figure 1, the carbazole moieties attached to both ends of the molecule are nearly perpendicular to the plane of the oligofluorene moiety. Therefore, π -electron delocalization between those units will be negligible. However, in their HOMO and LUMO orbitals the π -electrons are able to delocalize over the whole oligofluorene backbone and end-capped carbazole moieties through the lone electron pair of the nitrogen of the carbazole.

The optical properties of the *N*-carbazole-capped oligofluorenes CF_n ($n=1-3$) in chloroform are shown in Figure 2 and Table 1. The UV–vis absorption spectra

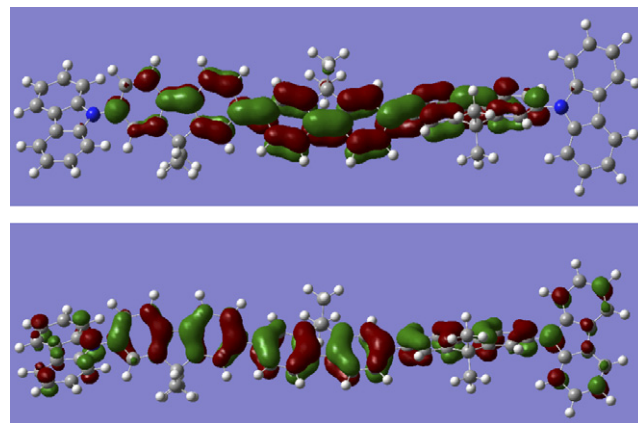


Figure 1. HOMO (bottom) and LUMO (top) of model CF_3 .

of CF_n ($n=1-3$) normalized at 294 nm are dominated by two major absorption bands, the less intense band around 294 nm being assigned to the $\pi-\pi^*$ local excitation of carbazole moieties at the terminal ends and the strong absorption band at longer wavelength corresponding to the $\pi-\pi^*$ electron transfer of the entire conjugated backbone. The intensities and absorption maxima of the latter band progressively increased as the number of the fluorene units per molecule increased. This result can be explained in terms of the decreasing HOMO–LUMO energy gap as delocalization of the

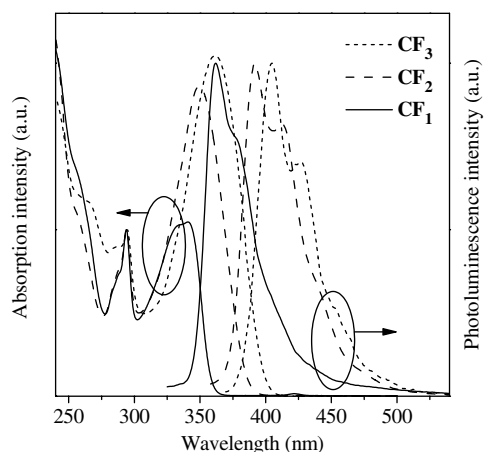


Figure 2. UV-vis absorption and photoluminescence spectra of CF_n ($n = 1-3$) measured in dilute CHCl_3 solution.

π -electron system along the backbone is extended. In comparison to the absorption maxima of their corresponding oligofluorenes, the absorption maxima of CF_n ($n = 1-3$) were about 8–20 nm red-shifted. This indicates that there is π -conjugation through the lone electron pair at the nitrogen atom of the carbazole units and that the π -electrons are delocalized over the entire conjugated backbone as indicated by the quantum chemical calculation results. The photoluminescence (PL) spectra of CF_n ($n = 1-3$) exhibited strong emission in the blue region with the emission maxima being gradually red-shifted with respect to an increase of the π -conjugation length of the fluorescent cores as observed in the absorption spectra. Upon excitation either at 350 nm corresponding to the absorption of the oligofluorene cores or at 294 nm due to the carbazole units, the resulting emission spectra obtained were identical. This suggests that energy or exciton can efficiently transfer from the peripheral carbazole via the lone electron pair of the nitrogen atom to the oligofluorene backbone.

The electrochemical properties of these newly synthesized end-capped oligomers are shown in Figure 3 and summarized in Table 1. Compounds CF_n ($n = 1-3$) exhibit two, three, and four chemically reversible oxidation processes, respectively. The first oxidation process can be attributed to the removal of electrons from the peripheral carbazole moieties and other reversible oxidation processes corresponding to the removal of electrons from the interior oligofluorene backbone. During the successive oxidation cycles of all compounds a slight shift of the CV curves was observed indicating a weak oxidative coupling at the 3,6-positions of the peripheral carbazole moieties (Fig. 4). This is usually detected in most carbazole derivatives with open 3,6-positions. The first oxidation potential of CF_n ($n = 1-3$) is not significantly affected by the number of fluorene units within the core as the oxidation occurs only at the end-capped carbazole units. Moreover, these oxidation potential values are slightly smaller than that of carbazole

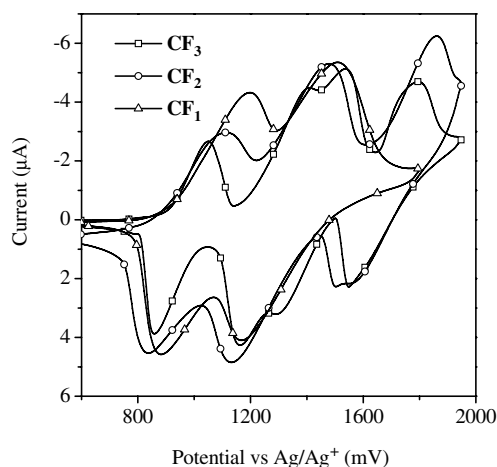


Figure 3. CV curves of CF_n ($n = 1-3$) measured in CH_2Cl_2 at a scan rate of 100 mV/s.

Table 1. Summary of the physical measurements of CF_n ($n = 1-3$)

Compound	$\lambda_{\text{abs}}^{\text{a}}$ (nm)	$\lambda_{\text{lum}}^{\text{b}}$ (nm)	E_{g}^{c} (eV)	$E_{1/2}/\Delta E^{\text{d}}$ (V)	$T_{\text{g}}/T_{\text{m}}/T_{\text{d}}^{\text{e}}$ ($^{\circ}\text{C}$)	HOMO ^f (eV)	LUMO ^g (eV)
CF_1	340	361	3.45	0.51/0.31 0.85/0.33	60/118/350	5.28	1.83
CF_2	349	391	3.20	0.46/0.25 0.81/0.33 1.21/0.27	69/196/425	5.28	2.08
CF_3	360	414	3.09	0.45/0.22 0.79/0.28 0.93/0.23 1.17/0.26	71/NA/427	5.32	2.23

^a Measured in dilute chloroform solution.

^b Excited at the absorption maxima.

^c Estimated from the onset of absorption ($E_{\text{g}} = 1240/\lambda_{\text{onset}}$).

^d Measured using a glassy carbon electrode as a working electrode, a platinum rod as a counter electrode, and SCE as a reference electrode in CH_2Cl_2 containing 0.1 M tetrabutylammonium hexafluorophosphate as a supporting electrolyte at a scan rate of 100 mV/s. All the potentials were calibrated with ferrocene, $E_{1/2}(\text{Fc}/\text{Fc}^+) = 0.47$ V ($\Delta E = 0.16$ V) versus SCE.

^e Obtained from DSC measurements with a heating rate of 10 $^{\circ}\text{C}/\text{min}$ under N_2 .

^f Calculated using the empirical equation: $\text{HOMO} = (4.44 + E_{\text{ox}}^{\text{onset}})^{17}$.

^g Calculated from $\text{LUMO} = \text{HOMO} - E_{\text{g}}$.

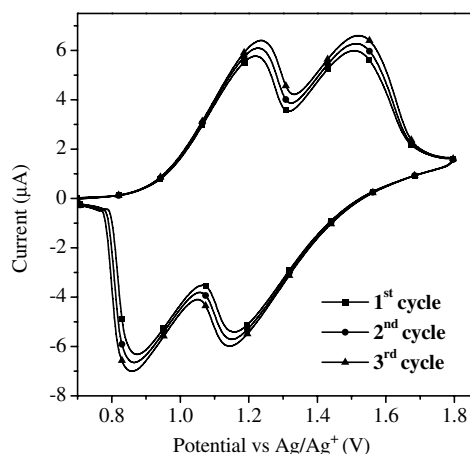


Figure 4. The successive CV curves of CF_1 measured in CH_2Cl_2 at a scan rate of 100 mV/s.

($E_{1/2} = 1.09$ V), indicating that the incorporation of carbazole at the terminal ends makes the resulting molecules more susceptible to electrochemical oxidation. The HOMO and LUMO energy levels were estimated from the absorption onset and the onset oxidation potential and are listed in Table 1. The results reveal that with the incorporation of dicarbazole end-caps, the HOMO energy level of the oligofluorenes moves up to ~ 5.32 eV (relative to the vacuum level). Such a high-lying HOMO energy level greatly reduces the energy barrier for hole injection from indium thin oxide (ITO) ($\phi = 4.80$ eV) to the emissive Alq_3 ($\phi = 5.80$ eV). Accordingly, compounds CF_n ($n = 1-3$) can also be used as hole transport and injection materials for double-layer OLEDs.

Thermal analysis reveals that the oligomers CF_n ($n = 1-3$) are thermally stable with the onset of decomposition temperatures in the range of 350–427 °C under nitrogen. Differential scanning calorimetry (DSC) measurements show that both compounds CF_1 and CF_2 are semi-crystalline. Their glass transition temperatures (T_g) range from 60 to 69 °C (Table 1). Compound CF_3 behaves totally differently. Only the glass transition at about 71 °C can be seen on repeated DSC heating cycles with no crystallization or melting peaks observed. The ability of CF_3 to form a molecular glass and the possibility to prepare thin films from CF_3 both by evaporation and by solution casting are highly desirable for applications in OLEDs.

In conclusion, we have demonstrated an efficient synthetic method for the preparation of a series of *N*-carbazole end-capped oligofluorenes. Carbazole was attached at the C-9 position to both ends of the oligofluorenes via Ullmann coupling. The absorption and emission spectra were gradually red shifted when the number of fluorene units was increased. The oligomers exhibit excellent electrochemical reversibility with the first oxidation potential being essentially unaffected by the chain length extension. They are suitable blue light-emitting or hole-transporting materials for electroluminescent devices.

Acknowledgements

This research was supported by the National Metal and Materials Technology Centre (MTEC) of Thailand (Grant MT-S-46-POL-24-249-G). We also thank Chulabhorn Research Institute (CRI) of Thailand for HRMS measurements.

References and notes

1. Yasuda, T.; Fujita, K.; Tsutsui, T.; Geng, Y.; Culligan, S. W.; Chen, S. H. *Chem. Mater.* **2005**, *17*, 264–268.
2. Lee, S. H.; Tsutsui, T. *Thin Solid Films* **2000**, *363*, 76–80.
3. Kreyenschmidt, M.; Klaerner, G.; Fuhrer, T.; Ashenurst, J.; Karg, S.; Chen, W. D.; Lee, V. Y.; Scott, J. C.; Miller, R. D. *Macromolecules* **1998**, *31*, 1099–1103.
4. Zhou, X. H.; Yan, J.-C.; Pei, J. *Org. Lett.* **2003**, *5*, 3543–3546.
5. Wong, K. T.; Chien, Y. Y.; Chen, R. T.; Wang, C. F.; Lin, Y. T.; Chiang, H. H.; Hsieh, P. Y.; Wu, C. C.; Chou, C. H.; Su, Y. O.; Lee, G. H.; Peng, S. M. *J. Am. Chem. Soc.* **2002**, *124*, 11576–11577.
6. Geng, Y.; Trajkovska, A.; Katsis, D.; Ou, J. J.; Culligan, S. W.; Chen, S. H. *J. Am. Chem. Soc.* **2002**, *124*, 8337–8347.
7. Katsis, D.; Geng, Y. H.; Ou, J. J.; Culligan, S. W.; Trajkovska, A.; Chen, S. H.; Rothberg, L. J. *Chem. Mater.* **2002**, *14*, 1332–1339.
8. Li, Z. H.; Wong, M. S. *Org. Lett.* **2006**, *8*, 1499–1502.
9. Zhang, Q.; Chen, J. S.; Cheng, Y. X.; Geng, Y. H.; Wang, L. X.; Ma, D. G.; Jing, X. B.; Wang, F. S. *Synth. Met.* **2005**, *152*, 229–232.
10. Grazulevicius, J. V.; Strohmriegel, P.; Pielichowski, J.; Pielichowski, K. *Prog. Polym. Sci.* **2003**, *28*, 1297–1353.
11. Kotler, Z.; Segal, J.; Sigalov, M.; Ben-Asuly, A.; Khodorovsky, V. *Synth. Met.* **2000**, *115*, 269–273.
12. Kundu, P.; Thomas, K. R. J.; Lin, J. T.; Tao, Y.-T.; Chien, C.-H. *Adv. Funct. Mater.* **2003**, *13*, 445–451.
13. Van Dijken, A.; Bastiaansen, J. J. A. M.; Kiggen, N. M. M.; Langeveld, B. M. W.; Rothe, C.; Monkman, A.; Bach, I.; Stossel, P.; Brunner, K. *J. Am. Chem. Soc.* **2004**, *126*, 7718–7727.
14. Koene, B. E.; Loy, D. E.; Thompson, M. E. *Chem. Mater.* **1998**, *10*, 2235–2250.
15. Lee, J. K.; Klaerner, G.; Miller, R. D. *Chem. Mater.* **1997**, *11*, 1083–1088.
16. Characterization data for compounds, CF_1 : IR (KBr) 3045, 2926, 1597, 1450, 1230, and 748 cm^{-1} ; ^1H NMR (300 MHz, CDCl_3) δ 0.83 (6H, t, $J = 6.9$ Hz), 0.90–0.94 (4H, m), 1.18–1.28 (12H, m), 2.04–2.10 (4H, m), 7.30–7.37 (4H, m), 7.44–7.52 (8H, m), 7.61–7.65 (4H, m), 8.00 (2H, d, $J = 8.7$ Hz), and 8.20 (4H, d, $J = 7.7$ Hz); ^{13}C NMR (75 MHz, CDCl_3) δ 14.0, 22.5, 24.1, 29.6, 31.6, 40.2, 55.7, 109.8, 119.9, 120.4, 121.0, 121.9, 123.4, 125.9, 126.0, 136.8, 139.6, 141.0, and 152.9; HRMS-ESI m/z : [MH^+] calcd for $\text{C}_{49}\text{H}_{49}\text{N}_2$ 665.3890; found, 665.3888.
Compound CF_2 : IR (KBr) 3057, 2926, 1597, 1463, 1230, 818, and 749 cm^{-1} ; ^1H NMR (300 MHz, CDCl_3) δ 0.83 (12H, t, $J = 7.2$ Hz), 0.87–0.92 (8H, m), 1.17–1.22 (24H, m), 2.07–2.18 (8H, m), 7.32–7.37 (4H, m), 7.44–7.51 (8H, m), 7.59–7.61 (4H, m), 7.72 (2H, s), 7.75 (2H, d, $J = 8.1$ Hz), 7.90 (2H, d, $J = 7.8$ Hz), 7.97 (2H, d, $J = 7.4$ Hz), and 8.20 (4H, d, $J = 8.4$ Hz); ^{13}C NMR (75 MHz, CDCl_3) δ 14.0, 22.6, 23.9, 29.6, 31.5, 40.3, 55.6, 109.8, 119.9, 120.2, 120.4, 120.9, 121.5, 121.9, 123.4, 125.9, 125.9, 126.4, 136.4, 139.6, 140.1, 140.7, 151.9, and 152.9;

HRMS-ESI m/z : $[MH^+]$ calcd for $C_{74}H_{81}N_2$ 997.6394; found, 997.6409.

Compound **CF₃**; IR (KBr) 3056, 2928, 1597, 1461, 1233, 817, and 746 cm^{-1} ; 1H NMR (300 MHz, $CDCl_3$) δ 0.81–0.89 (30H, m), 1.17 (36H, br), 2.11–2.20 (12H, m), 7.32–7.37 (4H, m), 7.45–7.52 (8H, m), 7.59–7.60 (4H, m), 7.72–7.78 (8H, m), 7.87–1.92 (4H, m), 7.97 (2H, d, $J = 8.7$ Hz), and 8.21 (4H, d, $J = 7.6$ Hz); ^{13}C NMR (75 MHz, $CDCl_3$)

δ 14.0, 23.8, 31.5, 40.2, 55.6, 109.8, 119.8, 120.0, 120.1, 120.4, 120.9, 121.5, 121.9, 123.4, 125.8, 125.9, 126.2, 126.3, 136.3, 139.5, 140.1, 140.4, 140.9, 141.1, 151.8, 151.9, and 152.9; HRMS-ESI m/z : $[MH^+]$ calcd for $C_{99}H_{113}N_2$ 1329.8898; found, 1329.8912.

17. Meng, H.; Zheng, J.; Lovinger, A. J.; Wang, B.-C.; Van Patten, P. G.; Bao, Z. *Chem. Mater.* **2003**, *15*, 1778–1787.